ISSN 1062-8738, Bulletin of the Russian Academy of Sciences: Physics, 2026, Vol. 90, No. 2, pp. 260–265. © Pleiades Publishing, Ltd., 2026.

Raman Scattering in Lightly Doped Manganites $(La,Ca)Mn_{0.98}Fe_{0.02}O_3$

S. V. Zaitsev[a], *, V. D. Sedykh[a], and K. P. Meletov[a]

[a] *Osipyan Institute of Solid-State Physics of the Russian Academy of Sciences, Chernogolovka, Moscow oblast, 142432 Russia*

**e-mail: szaitsev@issp.ac.ru*

Received October 17, 2025; revised October 20, 2025; accepted October 27, 2025

Abstract—Polycrystalline samples of lightly doped manganite $La_{1-x}Ca_xMn_{0.98}Fe_{0.02}O_{3+\delta}$ ($x = 0.05$, 0.1, 0.2) were studied by Raman scattering. With increasing calcium content, the optical LO phonon bands, expressed only in samples of stoichiometric composition ($\delta = 0$, rhombic phase), are significantly weakened and broadened. In individual crystallites (~20%) of the sample with $x = 0.05$, the temperature dependences of the phonon $\nu \approx 610$ cm^{-1}, corresponding to symmetrical stretching of the MnO_6 octahedra, show softening below the magnetic ordering temperature $T \approx 120$ K. This indicates a strong coupling of the magnetic and phonon systems, as well as significant heterogeneity of the lightly doped samples.

Keywords: Raman scattering, doped manganite, structural phase separation

DOI: 10.1134/S1062873825715223

INTRODUCTION

Mixed valence oxides of the $R_{1-x}A_xMnO_3$ type, where R is a rare earth element and A is divalent Ca, Sr or Ba, have been the subject of scientific research for many decades [1, 2]. Strong interest in these compounds is caused by the manifestation of large values of negative magnetoresistance (NMR) in them [3, 4], charge and spin ordering effects depending on the Mn^{3+}/Mn^{4+} ratio [5, 6] and the similarity of many of their properties with the problem of high-temperature superconductivity in cuprates [7]. The most widely studied derivatives of the above general class of oxides are lanthanum manganite compounds with the general formula $La_{1-x}A_xMnO_3$. The end members of this series, namely $LaMnO_{3+\delta}$ and $AMnO_{3-\delta}$, where δ denotes the tendency of the manganese ions to be in the 3+ or 4+ valence state, represent two interesting classes of oxides. At room temperature, stoichiometric $LaMnO_3$ is orthorhombic due to the mismatch in the La–O and Mn–O bond lengths and the combined Jahn–Teller distortion associated with the Mn^{3+} ions. The system is antiferromagnetically ordered at $T_N = 135$ K, below which noncollinear distortions in the Mn^{3+} spin lattice lead to weak parasitic ferromagnetism. Changes in the crystallographic structure, as well as the magnetic and electrical properties of this system with increasing δ have been studied by many researchers [8–10]. Comprehensive studies in [8], for example, showed a rhombic phase for $0 < \delta < 0.06$ and a rhombohedral phase for $0.1 < \delta < 0.18$, with the system transitioning from an antiferromagnetic (AFM) and insulating state to a metallic ferromagnetic (FM) state through a spin glass phase with increasing δ. For $0.06 < \delta < 0.1$, a two-phase mixture of orthorhombic and rhombohedral phases was predicted [9, 10]. Detailed Mössbauer, X-ray and magnetic studies in [11, 12] showed phase separation in lightly doped lanthanum manganites of stoichiometric composition ($\delta = 0$). It represents the coexistence of three rhombic phases (*I*, *II* and *II**) with different types of magnetic ordering at low temperatures $T < 140$ K: phase *I* transitions to the FM, and phases *II* and *II** transition to the AFM state. At low temperatures, stoichiometric samples exhibit relaxation behavior, which may be due to the presence of small-sized magnetic clusters. Magnetic measurements also indicate the presence of a two-phase FM–AFM state at low temperatures.

Most of the information on the structure and phase stability of mixed $La_{1-x}A_xMnO_3$ oxides has been obtained using macroscopic methods such as X-ray and neutron diffraction, Mössbauer spectroscopy (Mössbauer spectroscopy is not a macroscopic method) or magnetic measurements. At the same time, studies of light transmission/absorption allow the study of electronic and phonon excitations, and Raman scattering (RS) of vibrational, magnetic and electronic excitations in these systems can become an additional powerful tool for studying structural and magnetic phase transformations depending on temperature and composition. RS has been widely used to study vibrational and magnetic excitations in various perovskites based on alkali halides [13], ternary iron and chromium oxides [14, 15] and undoped lantha-

num manganites $LaMnO_{3+\delta}$ of stoichiometric ($\delta = 0$) and non-stoichiometric ($\delta > 0$) compositions [16, 17]. Thus, RS study of unadoped lanthanum manganites $LaMnO_{3+\delta}$ showed the presence of the effect of giant softening of phonon modes below the Curie temperature [18]. In this case, the effect of softening of vibrational modes depends significantly on the stoichiometric composition (amount of oxygen) ($\delta > 0$) and the corresponding magnetic state. The study of the interaction of LO phonons with a magnetic system provides important information about the nature of the magnetic state [19]. At the same time, lightly doped lanthanum manganites $La_{1-x}A_xMnO_{3+\delta}$ ($x < 0.2$), prone to phase separation, have not been sufficiently studied [11, 12]. The use of micro-Raman spectroscopy allows the use of RS to detect and characterize small amounts of secondary phase that are below the detection limit of X-ray diffraction, as well as granular or polycrystalline micrometer-scale samples.

This work presents a systematic study of the Raman scattering in the calcium-lightly doped polycrystalline manganite $La_{1-x}Ca_xMn_{0.98}Fe_{0.02}O_{3+\delta}$ ($x = 0.05$, 0.1, 0.2) in a wide temperature range from 80 to 300 K, which covers the magnetic ordering temperature at $T \approx 120$ K. The results indicate a strong relationship between the magnetic and phonon subsystems, as well as significant heterogeneity of such samples.

EXPERIMENTAL

Polycrystalline samples were obtained by the sol–gel method from lanthanum and calcium nitrates, an aqueous solution of ^{57}Fe Mössbauer isotope nitrate and manganese acetate. Since the ionic radii of Mn^{3+} and Fe^{3+} are close to each other, such a substitution does not introduce noticeable structural distortions. The main synthesis was carried out in air at 1100°C for 10–20 h. Details of sample preparation, their composition and structure are described in [12]. To obtain a stoichiometric composition without excess oxygen ($\delta = 0$), $La_{1-x}Ca_xMn_{0.98}Fe_{0.02}O_{3+\delta}$ samples were annealed at $T = 650$°C in a vacuum (10^{-3} Torr). The samples are a conglomerate of melted particles ranging in size from fractions of a micrometer to tens of micrometers. Heat treatment does not significantly affect the change in particle size or appearance. According to iodometric titration data, the samples after vacuum annealing have a stoichiometric composition of $La_{1-x}Ca_xMn_{0.98}Fe_{0.02}O_3$.

To characterize the powder samples, X-ray diffraction patterns were recorded using a Siemens D-500 diffractometer ($CuK_{\alpha 1}$ and CoK_α radiation). The crystal lattice parameters were calculated using PowderCell software (Werner Kraus & Gert Nolze, BAM Berlin). X-ray structural data showed that in the studied samples at $x = 0.05$, the rhombic phase *II** (sp. gr. *Pnma*) is formed, and at $x = 0.10$ and 0.20, a mixture of two rhombic phases *II** and *I* (sp. gr. *Pnma*) appears [12]. Detailed Mössbauer studies indicated that the structural phase separation of a sample doped with 5% calcium at room temperature represents the coexistence of three orthorhombic phases: FM phase *I* (9%), and AFM phases *II* (56%) and *II** (35%) in the form of small-sized magnetic clusters [12]. With an increase in the Ca content, the relative content of the FM phase increases due to an increase in the amount of Mn^{4+} and the temperature of its magnetic transition increases.

Raman spectra were measured in backscattering geometry using a setup equipped with a home-made optical thermostat designed for Raman measurements in micro-samples from nitrogen temperature (≈80 K) to room one. The stabilization system ensures temperature maintenance accuracy of ±4°C. The optical part of the setup includes an Acton SpectraPro-2500i spectrograph with a cooled Pixis2K CCD detector and an Olympus BX51 microscope. A continuous solid-state single-mode laser with a wavelength of $\lambda = 532$ nm was used to excite the Raman scattering. Two different variants of cattle research were used: microscopic and macroscopic configurations. Polarization selection was not performed.

To study RS from individual grains of the polycrystalline powder, the laser beam was focused on a single grain of the sample using an Olympus SLMPLN objective with 50× magnification, a numerical aperture of 0.35, and a working distance of 18 mm (micro-configuration). The diameter of the focused laser spot was ≈3 μm, and the laser excitation power directly in front of the sample was ≈500 μW. In the macro-configuration on the polycrystalline powder, a laser spot of ≈100 μm in size and an excitation power of ≈20 mW was formed by means of lenses and a crossed slit. The laser line in the scattered beam was suppressed using an edge filter for $\lambda = 532$ nm with an absorbance of OD = 6 and a transmission band shift of ≈ 60 cm^{-1}. Temperature dependences were measured for two crystallites (samples no. 1 and no. 2) selected from a batch of the powdered polycrystalline sample $La_{1-x}Ca_xMn_{0.98}Fe_{0.02}O_3$ with $x = 0.05$.

RESULTS AND DISCUSSION

Figure 1 shows Raman spectra in the macro-configuration at $T = 300$ K for polycrystalline samples of the manganite $La_{0.95}Ca_{0.05}Mn_{0.98}Fe_{0.02}O_{3+\delta}$ both with a non-stoichiometric composition after synthesis in air ($\delta > 0$, rhombohedral crystal phase) and with a stoichiometric composition ($\delta = 0$) obtained after annealing in vacuum and having an orthorhombic phase. The classification of phonon modes in $LaMnO_3$ has been examined in numerous studies and is now fairly well established. Thus, the modes below 200 cm^{-1} in $LaFeO_3$ correspond to lattice vibrations of the heavy lanthanum ions, the modes in the 200–500 cm^{-1} range are associated with various vibrations of the

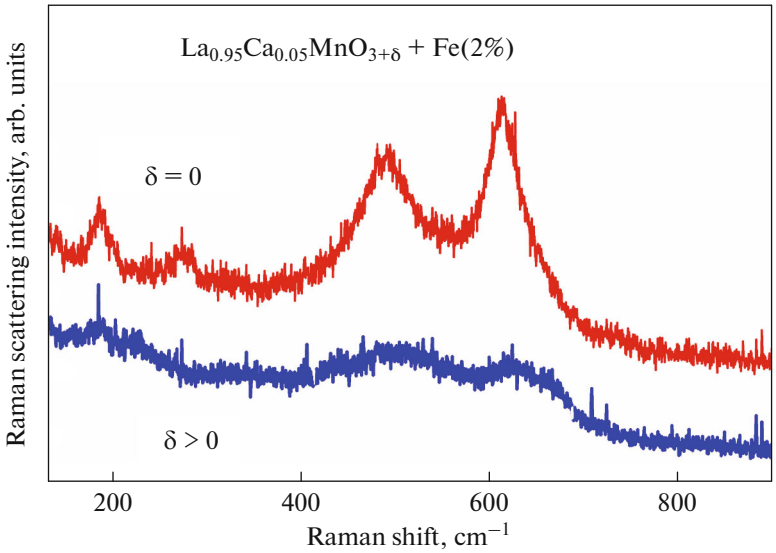

Fig. 1. Raman spectra at $T = 300$ K in the macro-configuration for polycrystalline samples of the $La_{0.95}Ca_{0.05}Mn_{0.98}Fe_{0.02}O_{3+\delta}$ manganite: nonstoichiometric composition after synthesis in air ($\delta > 0$) and stoichiometric composition after annealing in vacuum ($\delta = 0$).

lighter oxygen atoms in the tilted MnO_6 octahedra (≈490 cm^{-1} is the apical oxygen bending mode in the MnO_6 octahedra), and the most intense modes at ≈480 and ≈610 cm^{-1} are due to the antisymmetric and in-phase stretching of the in-plane Mn–O bonds [16]. Note that the modes at ≈480 cm^{-1} (antisymmetric stretching of the Mn–O bonds) and ≈490 cm^{-1} (apical bending mode of the MnO_6 octahedron) overlap and are poorly resolved in unpolarized measurements. In Fig. 1 it is seen that in the Raman spectrum of the stoichiometric sample two strong optical-phonon bands, $\nu_1 \approx 495$ cm^{-1} and $\nu_2 \approx 610$ cm^{-1}, dominate, whereas in the non-stoichiometric sample ($\delta > 0$) these bands are much weaker. Thus, the most significant differences are observed for the modes corresponding to vibrations in the MnO_6 octahedra.

In an ideal perovskite ABO_3 with cubic symmetry, with La ions in the A-site lattice positions and Mn ions at the centres of the oxygen octahedra (B sites), no phonon modes are Raman active. However, in most real perovskites the ions are displaced from their ideal cubic positions, which breaks the symmetry and leads to the appearance of LO phonons in the Raman spectra [20]. According to factor-group analysis, lifting the symmetry restriction yields substantially more allowed phonon modes for perovskite structures with orthorhombic distortions than with rhombohedral distortions [20]. This is exactly the situation in the studied samples (Fig. 1): the Raman intensity in the stoichiometric sample ($\delta = 0$) with the orthorhombic phase is much higher than in the non-stoichiometric sample ($\delta > 0$) with the rhombohedral phase [11, 12]. Below, we present the Raman-scattering results for $La_{1-x}Ca_xMn_{0.98}Fe_{0.02}O_{3+\delta}$ ($x = 0.05$, 0.1, 0.2) samples of stoichiometric composition ($\delta = 0$, orthorhombic phase).

With increasing calcium content, a strong decrease in intensity is observed, while the phonon bands shift to higher energy and broaden considerably (Fig. 2). Note that the phonon-energy shift is small, less than 7 cm^{-1} (<1 meV), whereas the linewidth increases by more than a factor of two. Similar spectral changes were reported for $LaMnO_3$ doped with another divalent cation (Sr) in [21]. If the broadening is naturally associated with an increase in microscopic disorder, then the energy shift is related to the conversion of a fraction of Jahn–Teller Mn^{3+} ions into Mn^{4+} upon doping with divalent Ca. Such doping weakens the noncollinear lattice distortions linked to the Jahn–Teller effect in stoichiometric $LaMnO_3$ manganite. Note that the measurements in Fig. 2a were performed in the micro-configuration, so a Lorentzian fit works better than a Gaussian one, as in the macro-configuration probing a large ensemble of grains in the polycrystalline powder.

The study of the temperature dependence of the strongest LO phonons $\nu_1 \approx 490$ cm^{-1} and $\nu_2 \approx 610$ cm^{-1} (MnO_6 octahedral vibration modes) in the stoichiometric sample doped with a low Ca concentration $x = 0.05$ showed that, in some crystallites, an increase in temperature leads to an upshift of the ν_2 band by $\Delta\nu \approx 5$ cm^{-1} in a narrow range $T = 100$–110 K (Fig. 3). Overall, temperature dependences were measured for two crystallites (samples no. 1 and no. 2) selected from the polycrystalline powder batch. The temperature dependence of the Raman spectrum was also mea-

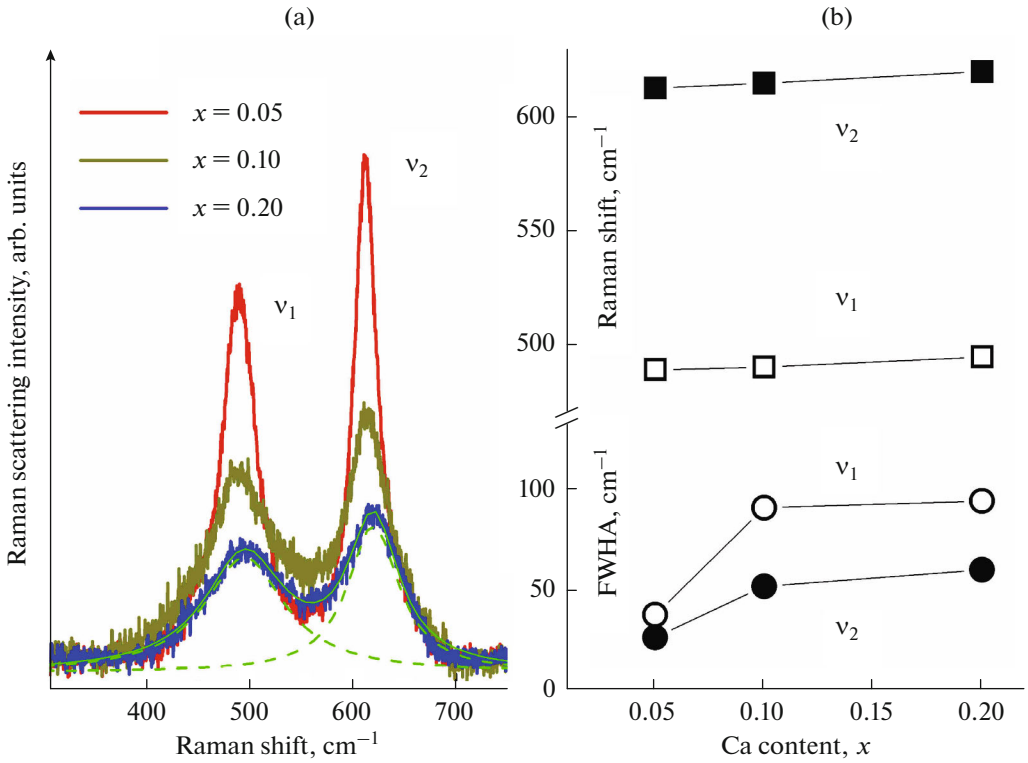

Fig. 2. (a) Raman spectra of stoichiometric samples ($\delta = 0$) with different calcium contents at $T = 300$ K after subtraction of a linear background. The dashed lines show a fit of the ν_1 and ν_2 phonons by two Lorentzians for $x = 0.2$. (b) Results of the Lorentzian fitting: peak position and full width at half maximum (FWHM) as a function of calcium content.

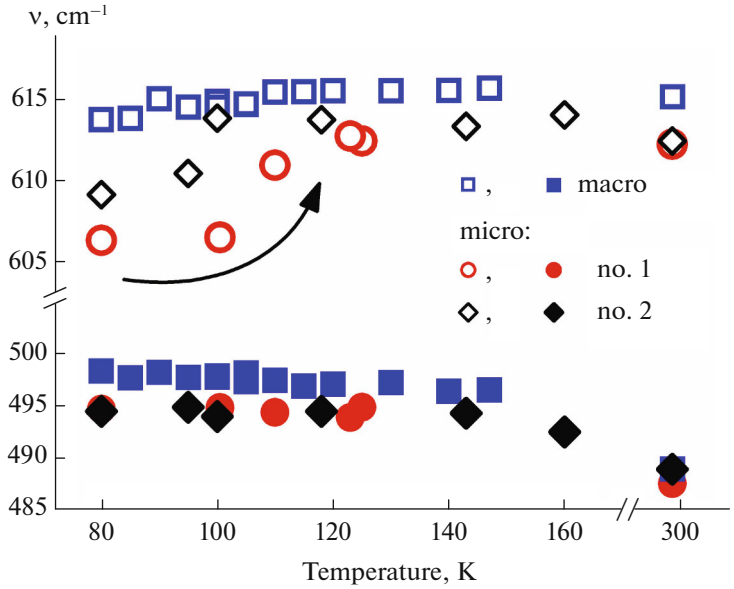

Fig. 3. Temperature dependence of the ν_1 and ν_2 phonons in the macro-configuration and in the micro-configuration (samples no. 1 and no. 2) (see text) for the stoichiometric ($\delta = 0$) lanthanum manganite sample doped with Ca at a concentration of $x = 0.05$.

sured for a large agglomerate of polycrystalline powder containing dozens of crystallites in the macro-configuration. The results are presented in Fig. 3. Note that, among the selected crystallites, only two out of ten (20%) showed a reduction in the ν_2-band energy (softening) by $\Delta\nu \approx 5$ cm^{-1} at liquid-nitrogen temperature compared with $T = 300$ K, and these were chosen for a more detailed study of the temperature dependence

of the Raman spectra. The temperature-induced upshift $\Delta\nu$ of the ν_2 band amounts to $\Delta\nu_2 \approx 6.5$ cm^{-1} in crystallite no. 1 (for $T = 100$–110 K) and $\Delta\nu_2 \approx 4.6$ cm^{-1} in crystallite no. 2 (for $T \approx 90$–100 K) in the micro-configuration (Fig. 3). For comparison, in the powder agglomerate as a whole there is only a weak monotonic increase of the ν_2-band energy, $\Delta\nu_2 < 2$ cm^{-1} over the wide temperature range from $T = 80$ K to 150 K (macro-configuration, Fig. 3). We also note that the temperature range of the ν_2-frequency shift differs between the two individual crystallites, indicating inhomogeneity of the lightly doped samples.

Turning to a discussion of the obtained results, we note that such anomalous behaviour of the phonon system—"softening" (decrease) of the LO-phonon frequencies below the FM or AFM transition temperature—is typical for doped and/or nonstoichiometric ($\delta > 0$) manganites $La_{1-x}A_xMnO_{3+\delta}$ (A = Ca, Sr, or Ba) [17, 18]. The point is that in manganites exhibiting strong distortions of the basic structural units, the MnO_6 octahedra (Jahn–Teller effect), a mode of strong coupling between the phonon, orbital, and magnetic subsystems is realized [22]. It is precisely this strong correlation between the lattice, spin, and electronic subsystems in lanthanum manganites that causes the decisive influence of the structure on all their physical properties (transport, magnetic, etc.) [3–7]. The most interesting and important is that, in the lightly Ca-doped ($x = 0.05$) manganite sample studied here, the "anomalous" temperature dependence of the mode energy is observed only for the $\nu_2 \approx 610$ cm^{-1} band, whereas the $\nu_1 \approx 490$ cm^{-1} band shows "standard" behaviour governed by anharmonic effects. Softening of the LO-phonon ν_1 with increasing temperature occurs in both cases, in the micro- and in the macro-configuration (Fig. 3).

The difference in the behaviour of the ν_1 and ν_2 phonon modes contrasts with that in the $(La,Sr)MnO_3$ system doped with another divalent cation (Sr) in [21], where the softening of ν_1 below $T_N \approx 150$ K was weaker than that of ν_2. Similar decoupled behaviour of the two MnO_6 octahedron modes—softening of ν_2 below $T_N = 128$ K and standard LO-phonon behaviour of the low-energy $\nu_1 \approx 490$ cm^{-1} mode—was also observed in undoped but nonstoichiometric ($\delta > 0$) $LaMnO_{3+\delta}$ manganite at small $\delta < 0.085$, when $LaMnO_{3+\delta}$ is in the AFM state [18]. With increasing $\delta \geq 0.085$, when $LaMnO_{3+\delta}$ transforms into the FM phase, an anomalously strong "softening" of the frequencies of both LO phonons is observed below the Curie temperature.

Thus, the most unusual temperature behaviour is exhibited by the ν_1 and ν_2 phonon modes in the sample with $x = 0.05$, which overall shows AFM behaviour: according to Mössbauer data, the relative fraction of the FM ortho-*I* phase at room temperature is less than 7% [12]. At low temperatures, stoichiometric samples display relaxation-type behaviour, which may be associated with the presence of small magnetic clusters. Magnetic measurements also indicate that at low temperatures a two-phase ferromagnetic–antiferromagnetic state is realized [23]. The Néel temperatures of the two AFM phases, determined from magnetic-susceptibility measurements, are $T_N \approx 121$ K (ortho-*II*) and $T_N \approx 130$ K (ortho-*II**) [23], which agrees well with the observed anomalies in the ν_2-phonon behaviour (Fig. 3). At the same time, the fact that such anomalous behaviour is seen only in a small fraction of grains in the polycrystalline powder (~20%) indicates substantial inhomogeneity of the lightly doped samples.

CONCLUSIONS

A detailed Raman scattering study of polycrystalline samples with a low content of dopant in stoichiometric manganite $La_{1-x}Ca_xMn_{0.98}Fe_{0.02}O_{3+\delta}$ ($x = 0.05$, 0.1, 0.2) has shown the following. With increasing calcium content, the optical LO-phonon bands, which are pronounced only in stoichiometric samples ($\delta = 0$, orthorhombic phase), become strongly weakened and significantly broadened; the temperature dependences of the phonon associated with symmetric stretching of the MnO_6 octahedra ($\nu \approx 610$ cm^{-1}) display a softening of $\Delta\nu \approx 5$ cm^{-1} in individual crystallites (~20%) of the $x = 0.05$ sample below its AFM ordering temperature $T_N \approx 120$ K.

These results indicate strong coupling between the magnetic and phonon subsystems, as well as substantial inhomogeneity in the lightly doped samples.

FUNDING

The work was carried out within the framework of the state assignment of the Osipyan Institute of Solid-State Physics of the Russian Academy of Sciences.

CONFLICT OF INTEREST

The authors of this work declare that they have no conflicts of interest.

REFERENCES

1. Jonker, G.H. and van Santen, J.H., *Physica*, 1950, vol. 16, no. 3, p. 337.
2. Zener, C., *Phys. Rev.*, 1951, vol. 82, p. 403. https://doi.org/10.1103/PhysRev.82.403
3. von Helmolt, R., Wecker, J., Holzapfel, B., et al., *Phys. Rev. Lett.*, 1993, vol. 71, p. 2331. https://doi.org/10.1103/PhysRevLett.71.2331
4. Jin, S., McCormack, M., Tiefel, T.H., and Ramesh, R., *J. Appl. Phys.*, 1994, vol. 76, p. 6929. https://doi.org/10.1063/1.357711

5. Yoshizawa, H., Kawano, H., Tomioka, Y., and Tokura, Y., *Phys. Rev. B*, 1995, vol. 52, p. R13145. https://doi.org/10.1103/PhysRevB.52.R13145
6. Goodenough, J.B., *Phys. Rev.*, 1967, vol. 164, p. 785. https://doi.org/10.1103/PhysRev.164.785
7. Khomskii, D.I. and Sawatzky, G.A., *Solid State Commun.*, 1997, vol. 102, p. 87. https://doi.org/10.1016/S0038-1098(96)00667-4
8. Töpfer, J. and Goodenough, J.B., *J. Solid State Chem.*, 1997, vol. 130, p. 117.
9. Hauback, B.C., Fjellvåg, H., and Sakai, N., *J. Solid State Chem.*, 1996, vol. 124, p. 43.
10. Verelst, M., Rangavittal, N., Rao, C.N.R., and Rousset, A., *J. Solid State Chem.*, 1993, vol. 104, p. 74.
11. Pchelina, D.I., Medvetskaya, I.Y., Chistyakova, N.I., et al., *J. Surf. Investig.*, 2018, vol. 12, no. 6, p. 1047.
12. Pchelina, D.I., Medvetskaya, I.Y., Chistyakova, N.I., et al., *J. Surf. Investig.*, 2019, vol. 13, p. 462.
13. Fleury, P.A., *J. Appl. Phys.*, 1970, vol. 41, p. 886. https://doi.org/10.1063/1.1658691
14. Udagawa, M., Kohn, K., Koshizuka, N., et al., *Solid State Commun.*, 1975, vol. 16, p. 779.
15. Venugopalan, S., Dutta, M., Ramdas, A.K., and Remeika, J.P., *Phys. Rev. B*, 1985, vol. 31, p. 1490. https://doi.org/10.1103/PhysRevB.31.1490
16. Iliev, M.N., Abrashev, M.V., Lee, H.-G., et al., *Phys. Rev. B*, 1998, vol. 57, p. 2872. https://doi.org/10.1103/PhysRevB.57.2872
17. Granado, E., Garcia, A., Sanjurjo, J.A., et al., *Phys. Rev. B*, 1999, vol. 60, p. 11879. https://doi.org/10.1103/PhysRevB.60.11879
18. Choi, K.-Y., Pashkevich, Yu.G., Gnezdilov, V.P., et al., *Phys. Rev. B*, 2006, vol. 74, p. 064406. https://doi.org/10.1103/PhysRevB.74.064406
19. Maksimov, A.A., Tartakovskii, I.I., Abdullaev, N.A., and Mamedov, N.T., *Bull. Russ. Acad. Sci.: Phys.*, 2025, vol. 89, no. 2, p. 276.
20. Chaitali, R. and Budhania, R.C., *J. Appl. Phys.*, 1999, vol. 85, p. 3124. https://doi.org/10.1063/1.369596
21. Choi, K.-Y., Lemmens, P., Sahaouriet, T., et al., *Phys. Rev. B*, 2005, vol. 71, p. 174402. https://doi.org/10.1103/PhysRevB.71.174402
22. Xu, J., Park, J.H., and Jang, H.M., *Phys. Rev. B*, 2007, vol. 75, p. 012409. https://doi.org/10.1103/PhysRevB.75.012409
23. Pchelina, D., Sedykh, V., Chistyakova, N., et al., *J. Phys. Chem. Solids*, 2021, vol. 159, p. 110268. https://doi.org/10.1016/j.jpcs.2021.110268

Translated by E. Domoroshchina